Materials Science and Engineering C 63 (2016) 125–130

Contents lists available at ScienceDirect

Materials Science and Engineering C

journal homepage: www.elsevier.com/locate/msec

In Vivo evaluation of adipogenic induction in fibrous and honeycomb-structured atelocollagen scaffolds

Andrea P. Rodríguez [a,c], Betiana Felice [c,*], María A. Sánchez [c], Hidetsugu Tsujigiwa [b], Carmelo J. Felice [c], Hitoshi Nagatsuka [a]

[a] Department of Oral Pathology and Medicine, Graduated School of Medicine and Dentistry, Okayama University, 2-5- 1 Shikata-cho, Okayama 7008558, Japan
[b] Department of Life Science, Okayama University of Science, 1-1 Ridai-cho, Kita-ku, Okayama 7000005, Japan
[c] Laboratorio de Medios e Interfases, Departamento de Bioingeniería, Universidad Nacional de Tucumán, Consejo Nacional de Investigaciones Científicas y Técnicas, Av. Kirchner 1800, Tucumán, Argentina T4000

ARTICLE INFO

Article history:
Received 16 September 2015
Received in revised form 7 January 2016
Accepted 19 February 2016
Available online 22 February 2016

Keywords:
Adipose tissue engineering
White adipocytes
Myogenic origin
Atelocollagen
In vivo

ABSTRACT

Nowadays, soft tissue restoration techniques are mainly focused on volume regeneration instead of function recovering. So far, autologous fat transplant has been the most popular method although its multiple reported problems like volume and function loss. Adipose tissue engineering therefore emerges as a solution for development of biological substitutes for soft tissue which promotes not only volume regeneration but also function restoration with minimal consequences. Here we tested fibrous-structured atelocollagen (FSA) scaffolds and honeycomb atelocollagen (HCA) scaffolds for their ability to induce adipogenesis *in vivo*. Implants were subjected to histological and immunohistochemical assessment after 1, 2, and 4 weeks of implantation. Our studies showed that FSA scaffolds induced *in vivo* a markedly adipogenic response, whereas an acute inflammatory process was observed at HCA scaffolds without tissue regeneration detected within them. Our histological findings concerning FSA scaffolds clearly showed the presence of adipose-like tissue surprisingly composed by a mixture of brown-like and white-like adipocytes at week 2 whereas only white-like adipocytes at week 4. Subsequent positive Pax7 immunostaining at weeks 1 and 2 suggested the existence of a common myogenic progenitor shared by brown-like and white-like adipocytes observed. Then, in this work we present FSA scaffolds as a promising structure for brown and white adipose tissue engineering.

1. Introduction

Contour defects caused by tumor resection, trauma or congenital abnormalities have represented an interesting challenge for health sciences. Until recently, restoration strategies of natural tissue were not often the primary goal in reconstruction; rather, restoration of soft tissue aesthetic function was targeted in order to minimize anxiety and negative psychological feelings associated with disfigurement [1,2].

Autologous fat tissue has been so far the most used repairing material for soft tissue defects. Although its use is logical in its approach, this method has not been consistently successful in patients. When autologous fat tissue is transplanted from one location to the defect site, the common occurrence is significant resorption of transplanted tissue over time, resulting in 40–60% of graft volume loss [3–5]. Then, only small defects can be corrected with this repairing material, and even these limited applications require repeated procedures to maintain the desired volume [3]. Adipose Tissue Engineering (ATE) therefore emerged like a promising technique for development of biological substitutes which promote not only volume regeneration but also function restoration of soft tissues with minimal rejection.

Tissue regeneration by ATE is achieved not only by controlling cell sources and biochemical environment but also through suitable scaffolds, which are required for support, migration and proliferation of anchorage-dependent adipocytes and preadipocytes [2]. Scaffolds for ATE may be either synthetic or natural, regarding the biomaterial chosen for their construction. Up to date, synthetic scaffolds based on e.g. polylactic acid, hydrogels and poly(lactic-co-glycolic acid) have been used successfully in ATE [6–8]. Nevertheless, they have some disadvantages such as lack of mechanical integrity and stiffness mismatch compared to native tissue, lack of biodegradability or generation of acidic microenvironments upon degradation with eventual inflammatory reactions and implant rejection [9–11]. Therefore, biocompatibility and biomimeticity hold by natural scaffolds become a main advantage over aforementioned synthetic structures. Several natural biomaterials like e.g. fibrin, gelatin, hyaluronan and matrigel have been studied for such purpose [12–14]. However, collagen remains as the most widely used scaffold natural material for ATE given its ability to support adipogenesis from several cell sources [15–18]. An alternative collagen-based biomaterial with extremely low antigenicity is produced by telopeptide

* Corresponding author.
E-mail address: betiana_felice@yahoo.com.ar (B. Felice).

http://dx.doi.org/10.1016/j.msec.2016.02.055
0928-4931/

removal from natural collagen molecule and it is known as atelocollagen which has been used mainly for e.g. cartilage restoration, bone and connective tissue engineering [19–21]. Nevertheless, preliminary works of this group showed that atelocollagen scaffolds also enhanced bone and adipose tissue formation [22,23]. Therefore, in this study we investigate and systematically evaluate *in vivo* adipogenic induction ability of fibrous-structured atelocollagen (FSA) scaffolds and honeycomb atelocollagen (HCA) scaffolds as a first approach concerning adipose tissue restoration.

2. Materials and methods

2.1. Animals

Twelve 4-week-old male severe combined immunodeficient (SCID) mice were used in this study in accordance with the Guidelines for Animal Experiments at Graduate School of Medicine and Dentistry Okayama University, Japanese Government Animal Protection and Management Law (No. 105) and Japanese Government Notification on Feeding and Safekeeping of Animals (No. 6).

2.2. Intramuscular implantation and explantation

FSA and HCA scaffolds (Fig. 1) of $3 \times 3 \times 2$ mm^3 were used for this work (Koken, Japan). SCID mice were subjected to intramuscular anesthesia with Ketamine (Fuji Chemical Industry, Japan) and Dormitol (Meiji Seika, Japan). The skin of the legs was shaved and disinfected with 70% alcohol and iodine. Subsequently, the scaffolds were implanted into intramuscular pockets made by blunt dissection between *tibialis anterior* and *soleus* muscles. The animals were sacrificed with an overdose of ether at 1, 2, and 4 weeks after implantation. For hematoxylin–eosin (H&E) staining, specimens and surrounding tissues were removed, fixed by 4% paraformaldehyde. Then, the samples were embedded in paraffin, sectioned at 4 μm in thickness and finally stained.

2.3. Adipose tissue staining by Oil Red O

To assess adipogenic differentiation, lipid deposits were visualized through Oil Red O staining. Briefly, frozen sections were prepared by embedding implants in Tissue Tek (Sakura Finetek, USA) followed by specimen freezing in liquid nitrogen bath and trimming. Then, they were dried with warm air and embedded in 60% propanol for 2 min. Subsequently, sections were stained with 0.3% Oil Red O solution at 37 °C for 7 min, provided by Kayayama Chemical (Japan). The dye was washed out with 60% propanol for 2 min. Thereafter, sections were rinsed in distilled water, stained with Mayer's hematoxylin and mounted with Aqueous Mounting Medium.

2.4. Transmission Electron Microscopy (TEM)

TEM of implanted samples was performed by negative staining. Specimens and surrounding tissues were pre-fixed with 2.5% glutaraldehyde and 2% paraformaldehyde solution, post fixed with 1% osmium tetroxide dehydrated with a series of alcohols and infiltrated with resin. The resin sample block was trimmed, thin-sectioned thickness of 70 nm, and collected on formyar-coated copper grids. Before examining under the TEM, these grids were stained by uranyl acetate and lead citrate, followed by blotting with a filter paper and air drying. Samples were examined with Philips CM10 at 200 kV.

2.5. Immunohistochemical staining of CD34 and Pax7

The sections were immunostained with monoclonal antibodies against CD34 (abcam, UK) and Pax7 (Santa Cruz Biotechnology, USA) using Vectastain ABC Rat Kit method (Adivin-Biotin-peroxidase Complex, USA). The main steps were as follows: (1) inactivation of endogenous peroxidase with hydrogen peroxide in methanol for 30 min; (2) the activation of antigenicity was done with microwave treatment before blocking nonspecific protein binding with rabbit normal serum and horse normal serum, respectively, for 10 min at room temperature; (3) incubation with the primary antibody at 4 °C overnight. The optimal dilutions of each primary were (CD34) 1:100 and (Pax7) 1:200; (4) incubation with anti-rat IgG (1:200) and anti-mouse IgG (1:200), respectively, for 30 min; (5) incubation with ABC at a dilution of 1:50 for 30 min; and (6) treatment with DAB color development and counterstaining with Mayer's hematoxylin.

3. Results

3.1. Histological examination

In Vivo response to FSA and HCA scaffolds at weeks 1, 2 and 4 was initially studied through H&E staining. As it is observed in Fig. 2, low or no inflammatory reaction was noticed at FSA scaffold periphery and bulk. At week 1, spindle cells attached to FSA scaffold fibers were stained whereas at week 2 numerous rounded cells were colored. Some of them contained multiple cytoplasmic lipid droplets surrounding the nucleus, as it was confirmed by Oil Red O assay (Fig. 3). Strikingly, H&E assay revealed at week 4 the absence of such cells as well as the presence of white-like adipose tissue, composed by white-like adipocytes with single large cytoplasmic lipid droplets and flattened stained nucleus located on the cell periphery. Similar responses were observed at all FSA specimens.

Oppositely, no tissue regeneration at HCA specimens in addition to an acute inflammatory response at weeks 2 and 4 was observed (Fig. 4). Giant bodies stained at week 4 might indicate scaffold

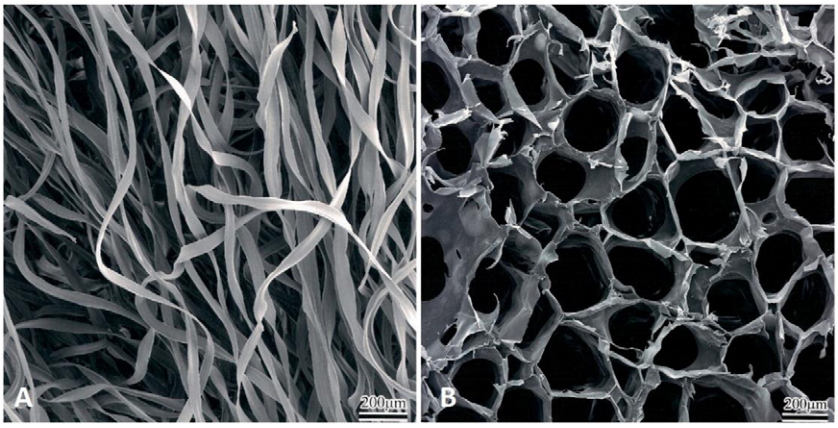

Fig. 1. SEM micrograph showing the (A) fibrillar microstructure of FSA scaffolds; and (B) honeycomb-like structure of HCA scaffolds.

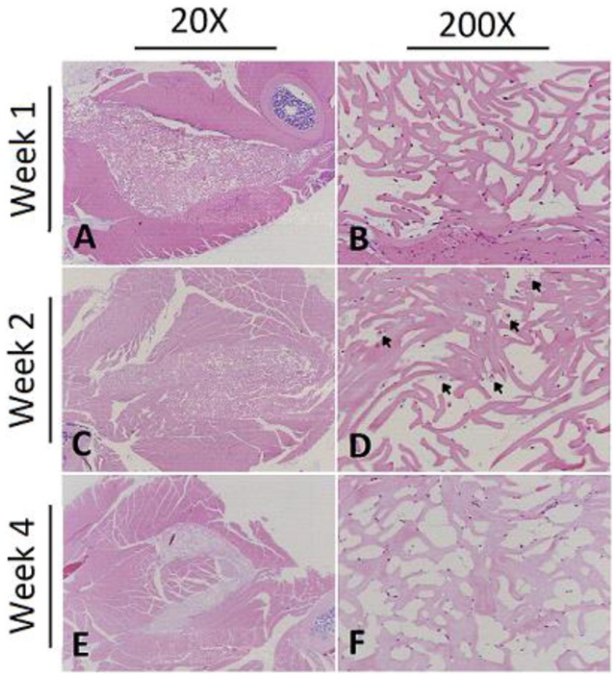

Fig. 2. Histological examination of implant specimens of FSA scaffolds at different weeks (Hematoxylin & Eosin staining). **(A and B) Week 1:** Note the presence of stained spindle cells attached to scaffold fibers. A weak inflammatory reaction is only seen at scaffold boundaries. **(C and D) Week 2:** Black narrows indicate brown-like adipocytes within the scaffold, with multiple cytoplasmic lipid droplets. Note the presence of some small spherical cells close to scaffold fibers. No inflammatory reaction is observed. **(E and F) Week 4:** Multiple white-like adipocytes within scaffold bulk are observed, with large cytoplasmic lipid droplets. Bars at the top of micrographs show respective magnifications.

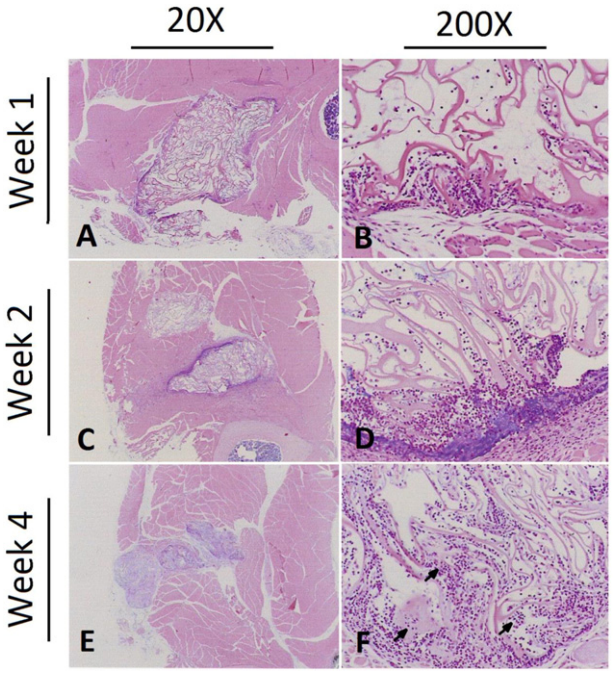

Fig. 4. Histological examination of implant specimens of HCA scaffolds at different weeks (Hematoxylin & Eosin staining). **(A and B) Week 1:** A markedly inflammatory reaction is observed mainly at scaffold periphery. Few spindle-like cells are only stained at scaffold borders. **(C and D) Week 2:** An acute inflammatory response at the periphery is observed. Some inflammatory cells are stained within scaffold bulk. **(E and F) Week 4:** Generalized inflammatory response is observed at the periphery as well as at scaffold bulk. Black arrows indicate giant bodies within scaffold bulk. Bars at the top of micrographs show respective magnifications.

degradation though cell phagocytosis. HCA scaffolds were negative stained for Oil Red O (data not shown).

3.2. TEM

Further analysis of cell features at week 2 in FSA specimens was performed by TEM. Surprisingly, sample exploration revealed two cell phenotypes at week 2: (1) brown-like adipocytes containing small cytoplasmic lipid droplets and numerous mitochondrias with abundant cristae (Fig. 5A); and (2) white-like adipocytes, with a single large cytoplasmic lipid droplet, few mitochondrias and a flattened nucleus located at cell periphery (Fig. 5B).

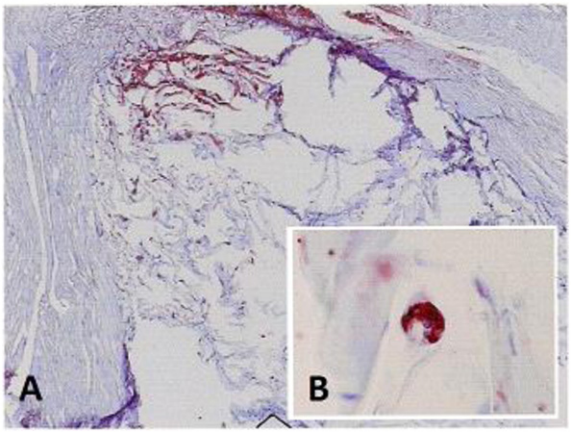

Fig. 3. Oil Red O staining of FSA scaffolds at week 2. **(A and B)** Multiple cytoplasmic lipid droplets within the cells are stained, as it is clearly shown at the zoomed micrograph.

3.3. Immunohistochemical examination

Immunohistochemical analysis was necessary in order to better understand former findings in FSA scaffolds. As shown in Fig. 6, Pax7 immunostaining revealed that such protein was expressed by spindle cells and brown-like adipocytes observed in FSA specimens at weeks 1 and 2 respectively. However, Pax7 assay was negative for white-like adipocytes in FSA scaffolds at week 4. HCA specimens, as it is shown in Fig. 6, were negative stained for Pax7 at weeks 1, 2 and 4.

Regarding CD34 immunoassay performed on FSA specimens, many endothelial cells in developing vessels at scaffold periphery were clearly positive with CD34 immunostaining at weeks 1, 2 and 4 according to Fig. 7. Contrastingly, angiogenesis processes were not observed within scaffolds bulk as the negative reaction for CD34 assay indicated. HCA specimens showed vessel development at scaffold periphery at weeks 1 and 2 as well. However, in contrast with FSA specimens, new vessels within HCA scaffold bulks were positive stained for CD34 at week 4, as it is shown in Fig. 7F.

4. Discussion

The major findings of the present study suggest, for the first time, that FSA scaffolds without pre-seeded cells successfully induce adipogenesis at intramuscular *in vivo* environment. Compared against HCA scaffolds, fibrous microstructure of FSA scaffolds definitively aroused as a key factor for adipogenic response development. H&E staining as wells as Oil Red O assay proved the existence of adipose-like tissue within FSA scaffold bulk. Strikingly, TEM micrographs revealed differences at the tissue cell composition between week 2 and 4, with a mixture of brown-like and white-like adipocytes at week 2 whereas at week 4 a clear predominance of white-like adipocytes. Latter observations in

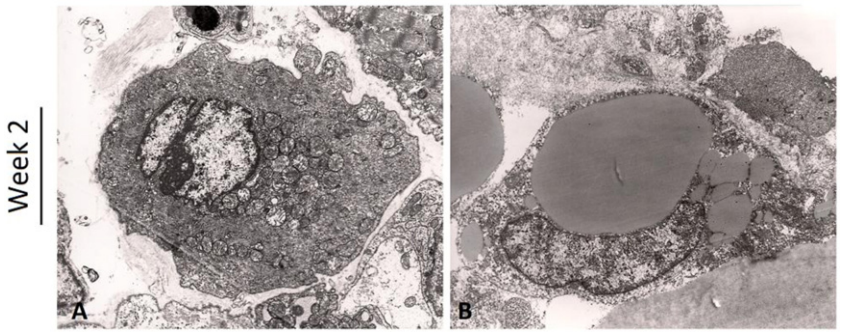

Fig. 5. TEM micrographs of cells observed within FSA scaffolds bulk at week 2. **(A)** Brown-like adipocyte containing numerous mitochondrias with abundant cristae and few and small cytoplasmic lipid droplets. **(B)** Early white-like adipocyte, with a large cytoplasmic lipid droplet surrounded by medium-size lipid droplets merging between each other. Observe the flattened nucleus close to the cell periphery.

addition to the positive Pax7 immunostaining of cells within FSA scaffolds at week 1 and 2 suggest a common myogenic progenitor shared by brown-like and white-like adipocytes.

For many years it was considered that Pax7 expression was restricted to myogenic cells and their muscular progeny given that it is a key protein for their survival and expansion [24–26]. However, Lepper et al. demonstrated that Pax7 is not exclusively expressed by these cells but also transiently by brown adipocytes during their early stages [27]. Subsequently, it was accepted a model arguing that brown adipocytes could be delineated from white adipocytes by their ancestral expression of myogenic proteins (*e.g.* Pax7, Myf5). Such theory was valid until the findings of Sánchez-Guraches et al., which clearly proved the existence of subsets of white adipocytes originated by myogenic lineages similar to those responsible for brown adipocytes proliferation [28,29]. Therefore, our results certainly support such approach regarding white and brown adipocytes common myogenic ancestors and suggest a migration of myosatellite cells from muscles surrounding the implants which subsequently gave rise to the observed adipocyte-like cells.

Regarding the observed cell composition differences, the apparently prevalence of white adipose tissue over brown at week 4 might have been induced by the lack of vascularization within FSA scaffolds bulk. It is known that white adipocytes grow up in hypoxic environments with low irrigation [30]. Furthermore, the enlarged they are the less irrigated they become [31]. In contrast, brown adipose tissue is highly vascularized containing many small capillaries which individually surround brown adipocytes so that to deliver anti-apoptotic molecules (*e.g.* norepinephrine), adequate amounts of oxygen and lipids necessary for heat production. Moreover, the delivery to the organism of the heat produced by brown adipocytes is equally dependent on the heated blood leaving the tissue [32,33]. Therefore, the lack of angiogenesis at scaffold bulk, shown by CD34 immunostaining, could have induced the enlarging of white-like adipocytes as well as apoptosis of brown-like adipocytes observed at week 2.

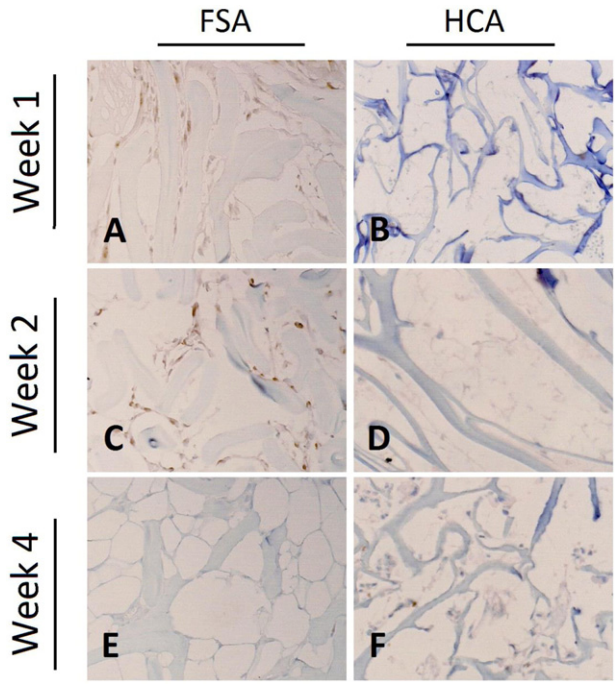

Fig. 6. Immunostaining for Pax7 of FSA scaffolds and HCA scaffolds at **(A and B)** week 1, (**C and D**) week 2 and **(E and F)** week 4. At FSA scaffolds note that spindle cells at week 1 and brown-like adipocytes at week 2 are positive stained for Pax7, whereas at week 4 all specimens were negative stained for such protein. HCA scaffolds were negative stained for Pax7 at all weeks.

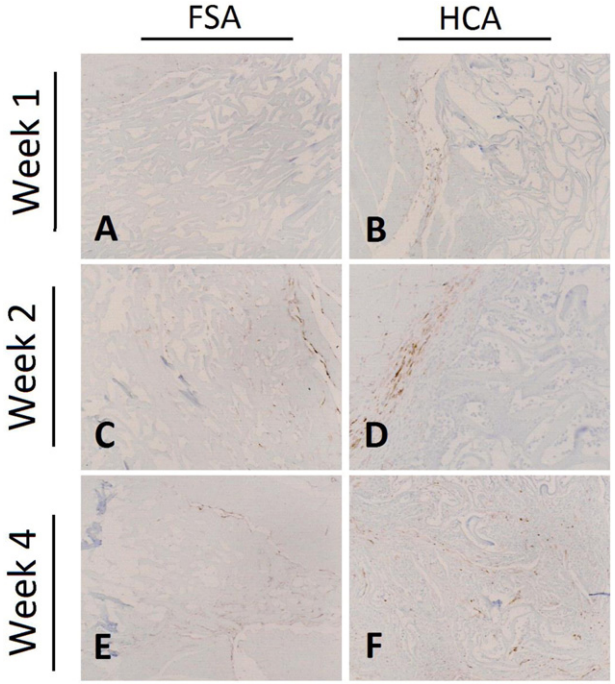

Fig. 7. Immunostaining for CD34 of FSA and HCA scaffolds at **(A and B)** week 1, (**C and D**) week 2 and **(E and F)** week 4. Positive staining exclusively at the periphery of FSA scaffolds and weeks 1, 2 and 4. Note the low vessel development within FSA scaffold bulk, considering the weak immunostaining inside the structures. HCA scaffolds show vessel development within scaffold bulk at week 4.

Positive adipogenic reaction at FSA scaffolds compared against negative adipogenic response for HCA scaffolds in addition to the acute inflammatory process observed clearly suggested that fibril organization of atelocollagen induced myosatellite-like cell migration followed by adipose tissue regeneration. Some authors demonstrated that myosatellite cells migration might be induced either by tissue injuring or by new fibrous tissue development [34,35]. However, as at HCA scaffolds there were no spindle-like cells observed in addition to negative Pax7 immunostaining, myosatellite-like cells migration induced by injured tissue could be discarded as hypothesis. Hence, fibril organization of FSA scaffolds arises as apparent cause of cell migration from surrounding muscles. Additionally, fibril organization might have induced myosatellite-like cells differentiation into adipocytes considering several studies which have shown that when preadipocytes differentiate into adipocytes, extracellular matrix goes from spiny to fibril organization [36,37]. Therefore, it can be assumed that fibril organization of FSA scaffolds might have induced the attraction of myosatellite-like cells, which consequently gave rise to generation of adipose tissue [23,24,26,32].

Finally it should be noted that even though SCID mice were used as experimental animals, an acute inflammatory response was observed at HCA scaffolds in contrast to a weak reaction at FSA scaffolds. Such response was also registered after subcutaneous implantation performed by this group during previous studies [23]. Therefore, this work demonstrates that scaffold structure is also an essential parameter which influences inflammatory reaction. However, further assays are necessary in order to systematically evaluate additional parameters *e.g.* porosity, mechanical properties and fibers diameter capable to modify inflammatory response.

5. Conclusion

In this study, we evaluated through histological and immunohistochemical techniques FSA and HCA scaffolds. Our results demonstrated FSA scaffold ability to induce adipogenesis *in vivo* without pre-seeded preadipocytes or adipogenic factors. Compared against HCA scaffolds, it was demonstrated that fibril organization of FSA scaffolds was a key factor for adipogenic response development. In addition, it was shown that the primary adipose tissue obtained at FSA scaffolds was composed by a mixture of brown and white adipocytes which arise from a common myogenic ancestor. Hence, FSA scaffolds demonstrated to be a promising structure for adipose tissue engineering.

Acknowledgments

Research conduction of this study was supported by the Japan Society for the Promotion of Science (19/07217, Japan). Article preparation was financed by the National Agency for Science and Technology (PICT 2009 n°87, Argentina).

References

[1] V.M. Hsu, C.A. Stransky, L.P. Bucky, I. Percec, Fat grafting's past, present, and future: why adipose tissue is emerging as a critical link to the advancement of regenerative medicine, Aesthet. Surg. J. 32 (2012) 892–899, http://dx.doi.org/10.1177/1090820X12455658.
[2] C.T. Gomillion, K.J.L. Burg, Stem cells and adipose tissue engineering, Biomaterials 27 (2006) 6052–6063, http://dx.doi.org/10.1016/j.biomaterials.2006.07.033.
[3] C.J. Tabit, G.C. Slack, K. Fan, D.C. Wan, J.P. Bradley, Fat grafting versus adipose-derived stem cell therapy: distinguishing indications, techniques, and outcomes, Aesthet. Plast. Surg. 36 (2012) 704–713, http://dx.doi.org/10.1007/s00266-011-9835-4.
[4] L. Flynn, K.A. Woodhouse, Adipose tissue engineering with cells in engineered matrices, Organogenesis 4 (2008) 228–235, http://dx.doi.org/10.4161/org.4.4.7082.
[5] S.J. Hong, J.H. Lee, S.M. Hong, C.H. Park, Enhancing the viability of fat grafts using new transfer medium containing insulin and β-fibroblast growth factor in autologous fat transplantation, J. Plast. Reconstr. Aesthet. Surg. 63 (2010) 1202–1208, http://dx.doi.org/10.1016/j.bjps.2009.05.040.
[6] J. Xu, Y. Chen, Y. Yue, J. Sun, L. Cui, Reconstruction of epidural fat with engineered adipose tissue from adipose derived stem cells and PLGA in the rabbit dorsal laminectomy model, Biomaterials 33 (2012) 6965–6973, http://dx.doi.org/10.1016/j.biomaterials.2012.06.010.
[7] M. Frydrych, S. Román, S. MacNeil, B. Chen, Biomimetic poly(glycerol sebacate)/poly(l-lactic acid) blend scaffolds for adipose tissue engineering, Acta Biomater. 18 (2015) 40–49, http://dx.doi.org/10.1016/j.actbio.2015.03.004.
[8] Y. Ogushi, S. Sakai, K. Kawakami, Adipose tissue engineering using adipose-derived stem cells enclosed within an injectable carboxymethylcellulose-based hydrogel, J. Tissue Eng. Regen. Med. 7 (2012) 884–892, http://dx.doi.org/10.1002/term.1480.
[9] K. Mäder, S. Nitschke, R. Stösser, H.-H. Borchert, A. Domb, Non-destructive and localized assessment of acidic microenvironments inside biodegradable polyanhydrides by spectral spatial electron paramagnetic resonance imaging, Polymer 38 (1997) 4785–4794, http://dx.doi.org/10.1016/S0032-3861(97)00003-7.
[10] J.H. Choi, J.M. Gimble, K. Lee, K.G. Marra, J.P. Rubin, J.J. Yoo, et al., Adipose tissue engineering for soft tissue regeneration, Tissue Eng. Part B Rev. 16 (2010) 413–426, http://dx.doi.org/10.1089/ten.teb.2009.0544.
[11] K. Hemmrich, D. von Heimburg, Biomaterials for adipose tissue engineering, Expert Rev. Med. Devices 3 (2006) 635–645, http://dx.doi.org/10.1586/17434440.3.5.635.
[12] A. Peterbauer-Scherb, M. Danzer, C. Gabriel, M. van Griensven, H. Redl, S. Wolbank, In vitro adipogenesis of adipose-derived stem cells in 3D fibrin matrix of low component concentration, J. Tissue Eng. Regen. Med. 6 (2011) 434–442, http://dx.doi.org/10.1002/term.446.
[13] E. Korurer, H. Kenar, E. Doger, E. Karaoz, Production of a composite hyaluronic acid/gelatin blood plasma gel for hydrogel-based adipose tissue engineering applications, J. Biomed. Mater. Res. A 00A (2013) 000-000.
[14] J.L. Kelly, M.W. Findlay, K.R. Knight, A. Penington, E.W. Thompson, A. Messina, et al., Contact with existing adipose tissue is inductive for adipogenesis in matrigel, Tissue Eng. 12 (2006) 2041–2047, http://dx.doi.org/10.1089/ten.2006.12.ft-111.
[15] D. Von Heimburg, M. Kuberka, R. Rendchen, K. Hemmrich, G. Rau, N. Pallua, Preadipocyte-loaded collagen scaffolds with enlarged pore size for improved soft tissue engineering, Int. J. Artif. Organs 26 (2003) 1064–1076.
[16] L. Wang, J.A. Johnson, Q. Zhang, E.K. Beahm, Combining decellularized human adipose tissue extracellular matrix and adipose-derived stem cells for adipose tissue engineering, Acta Biomater. 9 (2013) 8921–8931, http://dx.doi.org/10.1016/j.actbio.2013.06.035.
[17] C. Yu, J. Bianco, C. Brown, L. Fuetterer, J.F. Watkins, A. Samani, et al., Porous decellularized adipose tissue foams for soft tissue regeneration, Biomaterials 34 (2013) 3290–3302, http://dx.doi.org/10.1016/j.biomaterials.2013.01.056.
[18] K. Werner, M.G. Jakubietz, R.G. Jakubietz, K. Schmidt, C. Muhr, P. Bauer-Kreisel, et al., Toward reconstruction of the subcutaneous fat layer with the use of adipose-derived stromal cellseeded collagen matrices, Cytotherapy 16 (2014) 1700–1708, http://dx.doi.org/10.1016/j.jcyt.2014.06.007.
[19] V. Maier, C.M. Lefter, S.S. Maier, M. Butnaru, M. Danu, C. Ibanescu, et al., Property peculiarities of the atelocollagen-hyaluronan conjugates crosslinked with a short chain di-oxirane compound, Mater. Sci. Eng. C 42 (2014) 243–253, http://dx.doi.org/10.1016/j.msec.2014.05.027.
[20] Y. Tanaka, H. Yamaoka, S. Nishizawa, S. Nagata, T. Ogasawara, Y. Asawa, et al., The optimization of porous polymeric scaffolds for chondrocyte/atelocollagen based tissue-engineered cartilage, Biomaterials 31 (2010) 4506–4516, http://dx.doi.org/10.1016/j.biomaterials.2010.02.028.
[21] Y. Arima, N. Uemura, Y. Hashimoto, S. Baba, N. Matsumoto, Evaluation of bone regeneration by porous alpha-tricalcium phosphate/atelocollagen sponge composite in rat calvarial defects, Orthod. Waves 72 (2013) 23–29, http://dx.doi.org/10.1016/j.odw.2012.11.001.
[22] A.P. Rodríguez, L. Missana, H. Nagatsuka, M. Gunduz, H. Tsujigiwa, R. Rivera, et al., Efficacy of atelocollagen honeycomb scaffold in bone formation using KUSA/A1 cells, J. Biomed. Mater. Res. A 77A (2006) 707–717.
[23] A.P. Rodriguez, H. Tsujigiwa, S.S. Borkosky, P.P. Han, R. Tamamura, M. Gunduz, et al., Influence of three-dimensional scaffold on bone induction by KUSA/A1 cells, J. Hard Tissue Biol. 13 (2004) 5, http://dx.doi.org/10.2485/jhtb.13.91.
[24] F. Relaix, D. Rocancourt, A. Mansouri, M. Buckingham, A Pax3/Pax7-dependent population of skeletal muscle progenitor cells, Nature 435 (2005) 948–953, http://dx.doi.org/10.1038/nature03594.
[25] R. Sambasivan, R. Yao, A. Kissenpfennig, L. Van Wittenberghe, A. Paldi, B. Gayraud-Morel, et al., Pax7-expressing satellite cells are indispensable for adult skeletal muscle regeneration, Development 138 (2011) 3647–3656, http://dx.doi.org/10.1242/dev.073601.
[26] C. Lepper, T.A. Partridge, C.-M. Fan, An absolute requirement for Pax7-positive satellite cells in acute injury-induced skeletal muscle regeneration, Development 138 (2011) 3639–3646, http://dx.doi.org/10.1242/dev.067595.
[27] C. Lepper, C.M. Fan, Inducible lineage tracing of Pax7-descendant cells reveals embryonic origin of adult satellite cells, Genesis 48 (2010) 424–436, http://dx.doi.org/10.1002/dvg.20630.
[28] J. Sanchez-Gurmaches, C.M. Hung, C.A. Sparks, Y. Tang, H. Li, D.A. Guertin, PTEN loss in the Myf5 lineage redistributes body fat and reveals subsets of white adipocytes that arise from Myf5 precursors, Cell Metab. 16 (2012) 348–362, http://dx.doi.org/10.1016/j.cmet.2012.08.003.
[29] J. Sanchez-Gurmaches, D.A. Guertin, Adipocyte lineages: tracing back the origins of fat, Biochim. Biophys. Acta Mol. basis Dis. 2014 (1842) 340–351, http://dx.doi.org/10.1016/j.bbadis.2013.05.027.
[30] D.W. Fawcett, A comparison of the histological organization and cytochemical reactions of brown and white adipose tissues, J. Morphol. 90 (1952) 363–405.
[31] G.H. Goossens, The role of adipose tissue dysfunction in the pathogenesis of obesity-related insulin resistance, Physiol. Behav. 94 (2008) 206–218, http://dx.doi.org/10.1016/j.physbeh.2007.10.010.
[32] B. Cannon, Brown adipose tissue: function and physiological significance, Physiol. Rev. 84 (2004) 277–359, http://dx.doi.org/10.1152/physrev.00015.2003.
[33] S.R. Farmer, Molecular Determinants Of Brown Adipocyte Formation And Function Molecular Determinants Of Brown Adipocyte Formation And Function, 2008 1269–1275, http://dx.doi.org/10.1101/gad.1681308.

[34] J.L. Elster, C.R. Rathbone, Z. Liu, X. Liu, H.H. Barrett, R.P. Rhoads, et al., Skeletal muscle satellite cell migration to injured tissue measured with 111In-oxine and high-resolution SPECT imaging, J. Muscle Res. Cell Motil. 34 (2013) 417–427.
[35] H. Yin, F. Price, M.A. Rudnicki, Satellite cells and the muscle stem cell niche, Physiol. Rev. 93 (2013) 23–67, http://dx.doi.org/10.1152/physrev.00043.2011.
[36] S. Miettinen, J.R. Sarkanen, N. Ashammakhi, Adipose tissue and adipocyte, Top. Tissue Eng. 4 (2008) 1–26.
[37] N. Kawaguchi, C. Sundberg, M. Kveiborg, B. Moghadaszadeh, M. Asmar, N. Dietrich, et al., ADAM12 induces actin cytoskeleton and extracellular matrix reorganization during early adipocyte differentiation by regulating beta1 integrin function, J. Cell Sci. 116 (2003) 3893–3904, http://dx.doi.org/10.1242/jcs.00699.

Andrea P. Rodríguez is an assistant researcher in the National Scientific and Technical Research Council (CONICET, Argentina) and associate professor at Bioengineering Department in the National University of Tucumán (UNT, Argentina). She obtained her Ph.D. at the Department of Oral Pathology and Medicine, Graduate School of Medicine, Dentistry and Pharmaceutical Sciences, Okayama University, Japan. Her research interests include tissue engineering, cell culture and cell-biomaterial interactions.

Betiana Felice is currently a Doctoral Research Fellow with the National Scientific and Technical Research Council (CONICET, Argentina). She obtained her degree as Biomedical Engineer from the National University of Tucumán (Argentina). Her research interests include medical polymers applied to tissue engineering, antimicrobial systems and drug delivery in addition to electrospinning, TiO_2 as photocatalyst, cell culture, microbiology and nanotechnology.

María A. Sánchez is currently a Doctoral Research Fellow with the National Scientific and Technical Research Council (CONICET, Argentina). She obtained her degree as Biomedical Engineer from the National University of Tucumán (Argentina). Her research interests include surface treatment of titanium dioxide, osteo-active biomaterials, drug delivery, microbiology and nanotechnology.

Hidetsugu Tsujigiwa is currently a researcher and professor at the Okayama University of Science (Japan). He obtained his PhD degree at Okayama University (Japan). Hard tissue, stem cells and tissue regeneration have been for years his research fields. Nowadays, he is focused on the study of molecular mechanisms concerning tumor microenvironments toward non-invasive therapies development.

Carmelo J. Felice is a senior researcher at the National Scientific and Technical Research Council (CONICET, Argentina) and principal professor at Bioengineering Department in the National University of Tucumán (UNT, Argentina). His main research field is bioimpedancimetry applied to biosensors, neurophysiology and tissue engineering.

Hitoshi Nagatsuka is a senior researcher and professor at the Okayama University (Japan). Currently he is Chairman of the Oral Pathology Department (Okayama University, Japan) and responsible of numerous publications concerning bone tissue study and bone tissue regeneration.